Comparison of Technetium-99m-HMPAO and Xenon-133 Measurements of Regional Cerebral Blood Flow by SPECT

J. Kelly Payne, Madhukar H. Trivedi and Michael D. Devous, Sr.
Nuclear Medicine Center, The University of Texas Southwestern Medical Center, Dallas, Texas

This study compares ^{99m}Tc-HMPAO count ratios and derived regional cerebral blood flow (rCBF) to ^{133}Xe rCBF ratios and true rCBF (ml/min/100 g), respectively. **Methods:** Technetium-99m-HMPAO distribution was evaluated in 14 patients and 5 normal control subjects. Immediately after ^{133}Xe SPECT, subjects received 22 ± 4mCi ^{99m}Tc-HMPAO, and images were acquired 15 min after injection. rCBF (ml/min/100 g, ^{133}Xe) or regional count density (^{99m}Tc-HMPAO) were extracted from 24 ROI located 6 cm above the cantho-meatal line. These data were also normalized to global cerebral blood flow (gCBF) for ^{133}Xe or to global count density (gCD) for ^{99m}Tc-HMPAO. Technetium-99m-HMPAO ROI data also were expressed in units of ml/min/100 g by relating gCD to gCBF. Comparisons between ^{133}Xe and ^{99m}Tc-HMPAO were evaluated using a Bonferroni-corrected paired t-test and by linear regression analysis. **Results:** Profile plots demonstrated agreement in the pattern of relative distribution between rCBF ratios (^{133}Xe) and count density ratios (^{99m}Tc-HMPAO). Regression analysis indicated a significant correlation (r = 0.78), with a modest slope (0.52) and a large intercept (0.48). A closer correlation (r = 0.92) was found for the comparison between rCBF (^{133}Xe) and derived ^{99m}Tc-HMPAO rCBF. The slope was closer to one (0.82) and the intercept closer to zero. This relationship was also examined during high rCBF after a subset of these subjects (n = 7) was injected intravenously with 1 g acetazolamide. Again, profile plots and regression analysis demonstrated agreement in the pattern of distribution (ratios) between ^{133}Xe and ^{99m}Tc-HMPAO (r = 0.66). However, the slope was reduced and the intercept increased relative to resting data. Absolute flow correlations showed some improvement relative to the ratio data (r = 0.77). **Conclusion:** The distribution of ^{99m}Tc-HMPAO is linearly related to rCBF measured by ^{133}Xe SPECT, although our data suggest that ^{99m}Tc-HMPAO mildly underestimates rCBF above 80 ml/min/100 g. These results are similar to our previous comparison of ^{99m}Tc-ECD and ^{133}Xe.

Key Words: SPECT; technetium-99m-HMPAO; xenon-133; regional cerebral blood flow; acetazolamide

J Nucl Med 1996; 37:1735-1740

The study of regional cerebral blood flow (rCBF) by SPECT depends primarily on the ability of ^{99m}Tc- or ^{123}I-labeled imaging agents to distribute to target tissues in proportion to tissue perfusion and be retained long enough for tomographic imaging. However, dynamic measurement of rCBF using inert-gas tracers predates the use of static tracers. In fact, ^{133}Xe SPECT is the most well-established technique for the study of quantitative rCBF. It is, therefore, useful to compare new imaging agents against ^{133}Xe SPECT in determining their ability to follow rCBF. We have previously performed such a comparison for ^{99m}Tc ECD which showed that ^{99m}Tc ECD moderately overestimated low flow and moderately underestimated high flow (*1*).

Technetium-99m-HMPAO is an FDA-approved radiopharmaceutical that has been studied extensively as a marker of rCBF. Technetium-99m-HMPAO crosses the blood-brain barrier in proportion to rCBF, is retained approximately as a chemical microsphere and is stable in vivo for many hours (*2-4*). Technetium-99m-HMPAO, however, does not act as a perfect rCBF marker, principally because of backdiffusion of unmetabolized radiopharmaceutical from the brain (*3,4*). Models have been developed to quantitate rCBF using ^{99m}Tc-HMPAO that use a scale factor to account for backdiffusion at higher flow (*3-5*).

The current study compares ^{99m}Tc-HMPAO relative count density (normalized to whole-brain counts) to ^{133}Xe rCBF (ml/min/100 g) normalized to the average whole-brain flow and compares derived ^{99m}Tc-HMPAO rCBF (ml/min/100 g) and true rCBF (^{133}Xe). Finally, to investigate the relationship between ^{99m}Tc-HMPAO and rCBF at high rCBF, a subgroup of subjects was studied after the administration of a vasodilator (acetazolamide).

MATERIALS AND METHODS

Subjects

Subjects in this study included five neurologically and psychiatrically normal volunteers (2 men, 3 women, age 19–35 yr) and 14 patients with mild-to-moderate perfusion deficits. Patients ranged in age from 20 to 66 yr and included two men and seven women with major depressive disorder, one woman with Alzheimer's disease, one man with epilepsy, one man and one woman with migraine and one woman with stroke. In addition, 24–72 hr after the baseline study, all five normal subjects and two of these patients had repeat studies after an intravenous injection of 1 g acetazolamide. All subjects gave informed consent as approved by the Institutional Review Board of The University of Texas Southwestern Medical Center.

Kit Preparation

HMPAO Ceretec, Amersham was supplied in a rubber-stoppered vial, lyophilized, containing 0.5 mg exametazime [(RR,SS)-4,8-diaza-3,6,6,9-tetramethylundecane-2,10-dione bisoxime], 7.6 μg stannous chloride dihydrate and 4.5 mg sodium chloride sealed in a nitrogen atmosphere. Technetium-99m-HMPAO was prepared by mixing 30–50 mCi $^{99m}TcO_4^-$ (<2-hr old) into a vial of HMPAO. The solution was gently shaken and allowed to stand for 10 min before withdrawing the labeled compound for injection. All injections were made within 30 min of vial reconstitution. The radiochemical purity of ^{99m}Tc-HMPAO was tested according to the manufacturer's recommendations. In this study, only reconstituted kits with a radiochemical purity >80% were used.

Received Nov. 10, 1994; revision accepted Jan. 28, 1996.
For correspondence or reprints contact: Michael D. Devous, Sr., PhD, Nuclear Medicine Center, UT Southwestern Medical Center, 5323 Harry Hines Blvd., Dallas, TX 75235-9061.

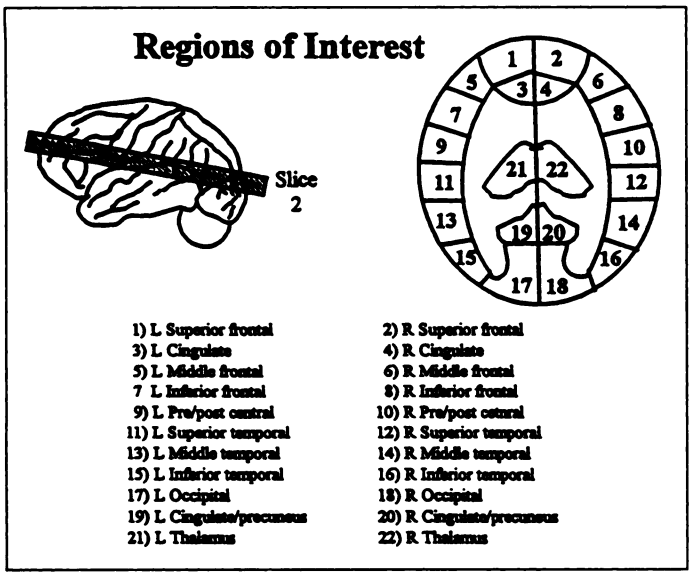

FIGURE 1. ROI designations within the slice 6 cm above the cantho-meatal line (CML, slice 2) and relative position of the slice within the brain.

Study Protocol

rCBF was determined by dynamic SPECT measurement of the cerebral transit of ^{133}Xe according to methods previously described using the Tomomatic 64 (Medimatic A/S, Copenhagen, Denmark) (*6*). At the time of the study, subjects were prepared by placing marks on the left side of the face using a template for positioning and measuring the head diameter (anterior to posterior and right to left) with calipers at 2 and 6 cm above and parallel to the cantho-meatal line (CML). Subjects were placed supine and positioned so that their heads were inside a plastic shield that lined the detection space and so that slices were obtained 2, 6 and 10 cm above and parallel to the CML (Fig. 1). A nose clip was placed to prevent exhalation of ^{133}Xe through the nasal cavities, and a mouth piece connected to the instrument was placed in the subject's mouth. After a 2-min adaptation period, subjects were administered 10–20 mCi/liter of ^{133}Xe in air for 1 min, followed by a 3-min washout period (*6*).

At the conclusion of the ^{133}Xe study, 22 ± 4 mCi ^{99m}Tc-HMPAO was administered intravenously, and the subject was removed from the camera field. The energy window of the Tomomatic 64 was adjusted for ^{99m}Tc, and a background was taken. After a 15-min postinjection delay, the subject was repositioned in the camera field in exactly the same position as the ^{133}Xe study. A 5-min static acquisition was conducted using the same high-sensitivity low-resolution collimators used for ^{133}Xe. Thus, the same slices at the same resolution were imaged for both ^{133}Xe and ^{99m}Tc-HMPAO in all subjects. A subset of subjects returned 24 to 72 hr after the baseline study and was injected intravenously with 1 g acetazolamide Diamox. After waiting 20 min, these subjects were studied as described above.

Image Reconstruction

Cross-sectional images of ^{133}Xe and ^{99m}Tc-HMPAO were reconstructed using filtered backprojection and were corrected for attenuation (*6*). Transverse resolution was 1.7 cm and axial resolution was 1.9 cm. Further, rCBF (ml/min/100 g) was calculated from ^{133}Xe SPECT data using the method of Kanno and Lassen (*7-9*). All images were displayed in 64 × 64 matrix using a linear 16-shade color scale, normalized to the highest flow value for ^{133}Xe or highest count density for ^{99m}Tc-HMPAO.

Data Analysis

rCBF (^{133}Xe) and ^{99m}Tc-HMPAO regional count density (rCD) were derived from 24 fixed regions of interest (ROIs) applied to the image 6 cm above the CML (Fig. 1) using the method of Stokely et al. (*10*). Regions were normalized to global cerebral blood flow (gCBF) for ^{133}Xe or to global count density (gCD) for ^{99m}Tc-HMPAO, derived from the average of values from all voxels in the left and right hemispheres in this slice. Profile plots were obtained of individual subjects and of average values for each region across subjects (mean ± s.d.). Data were analyzed for both individual regions and all regions combined. Comparisons between ^{133}Xe and ^{99m}Tc-HMPAO normalized data were evaluated for statistical significance using a Bonferroni-corrected paired t-test ($p < 0.0023$). Linear regression analysis was then used to examine the relationship between rCBF ratios and ^{99m}Tc-HMPAO count density ratios.

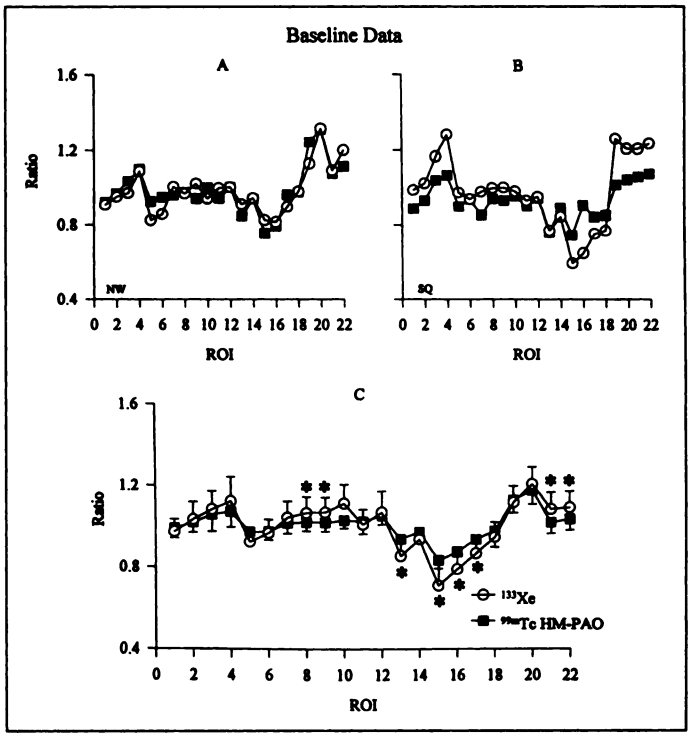

FIGURE 2. Profile plots comparing ^{99m}Tc-HMPAO count density ratios and rCBF (^{133}Xe) ratios for (A) one subject with a close relationship, (B) one subject with a weak relationship and (C) the relative distribution averaged across subjects. ROI numbers refer to the designations shown in Figure 1. *Areas of significant difference between ^{133}Xe and ^{99m}Tc-HMPAO.

In addition, to explore whether the relationship between rCBF (^{133}Xe) and ^{99m}Tc-HMPAO was dependent on absolute flow, ^{99m}Tc-HMPAO ROI data were expressed in units of ml/min/100 g assuming equivalency between gCBF (^{133}Xe) and gCD (^{99m}Tc-HMPAO). That is, for a given ROI, $rCBF_{HMPAO} = CD_{HMPAO}[(gCBF_{133_{Xe}})/(gCD_{HMPAO})]$. Linear regression analysis was then used to examine the relationship between rCBF (ml/min/100 g) and derived ^{99m}Tc-HMPAO rCBF (ml/min/100 g).

Linear regression analysis was also used to examine the relationship of rCBF ratios and ^{99m}Tc-HMPAO count density ratios and of derived ^{99m}Tc-HMPAO rCBF (ml/min/100 g) to that of true rCBF in the seven subjects imaged after vasodilation with Diamox. Finally, regression analysis was conducted on the total data set (baseline+Diamox).

RESULTS

Profile plots comparing rCBF (^{133}Xe) ratios and ^{99m}Tc-HMPAO count density ratios during a baseline study for one subject with a close relationship is shown in Figure 2A and for one subject with a weak relationship in Figure 2B. The relative distribution of the two radiopharmaceuticals averaged across subjects is shown in Figure 2C. The distribution across regions

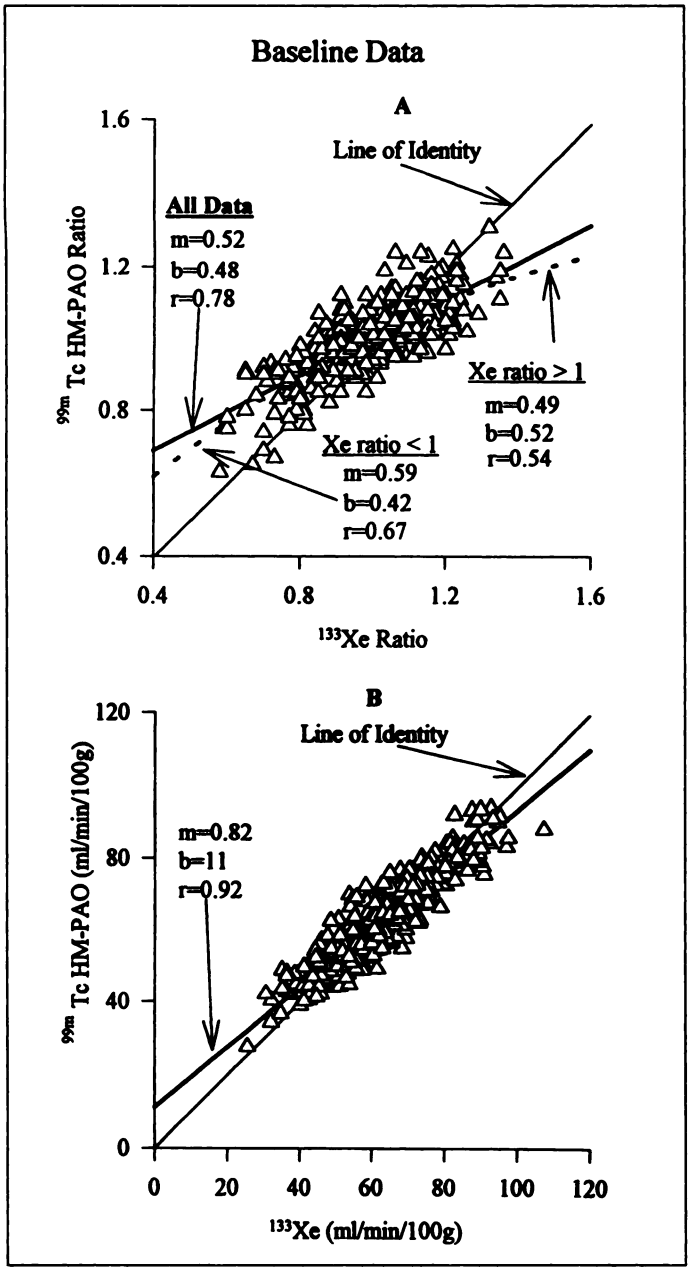

FIGURE 3. (A) Linear regression analysis comparing ^{99m}Tc-HMPAO count density ratios to rCBF ratios. Solid line represents a regression for the whole dataset. Dashed line represents the split regressions for data above and below a ^{133}Xe rCBF ratio of 1 or (B) regression analysis comparing derived ^{99m}Tc-HMPAO rCBF (ml/min/100 g) to rCBF (ml/min/100 g, ^{133}Xe).

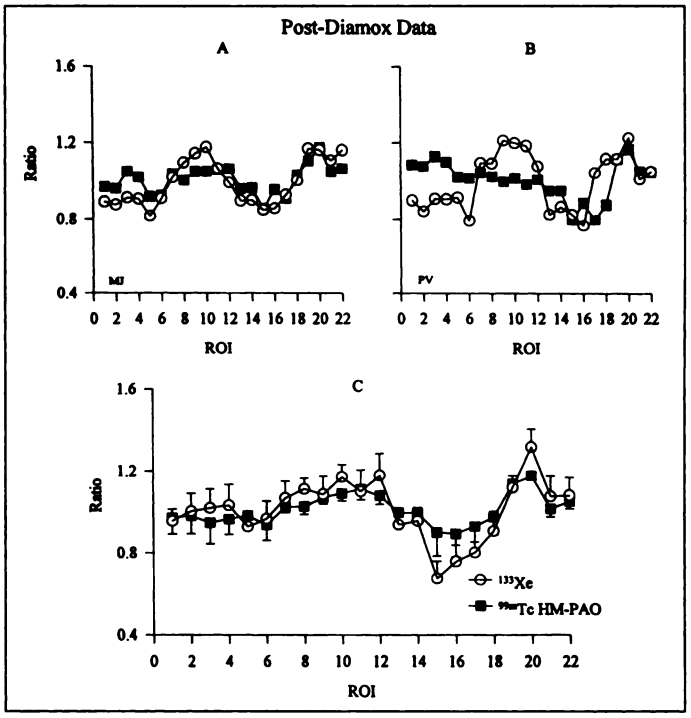

FIGURE 4. Profile plots comparing ^{99m}Tc-HMPAO count density ratios and rCBF (^{133}Xe) ratios after Diamox for (A) one subject with a close relationship, (B) one subject with a weak relationship and (C) the relative distribution averaged across subjects.

for all subjects was not significantly different between ^{133}Xe and ^{99m}Tc-HMPAO ($p = 0.52$). However, there were eight individual ROIs that showed significant differences between ^{133}Xe and ^{99m}Tc-HMPAO (Fig. 2C).

The results of linear regression analysis comparing rCBF ratios to ^{99m}Tc-HMPAO count density ratios is shown in Figure 3A. A significant correlation was observed ($r = 0.78$) with a slope of 0.52 ± 0.02 and intercept of 0.48 ± 0.02. Since ^{99m}Tc-HMPAO has been reported to underestimate high rCBF (*4*), we also performed separate regressions on low ratio data (^{133}Xe ratio > 1) and high ratio data (^{133}Xe ratio ≥ 1). A decrease in the correlation ($r = 0.54$) was seen in the high ratio dataset but the slope (0.49 ± 0.05) and the intercept (0.52 ± 0.06) were not different from those for the combined data. The correlation coefficient for the low ratio data set ($r = 0.67$) was slightly less than that for the complete data. The slope (0.59 ± 0.05) was moderately higher and the intercept (0.42 ± 0.04) was slightly lower.

Results of regression analysis comparing rCBF (ml/min/100 g, ^{133}Xe) to derived ^{99m}Tc-HMPAO rCBF (ml/min/100 g) is shown in Figure 3B. A closer correlation ($r = 0.92$) was found for these data than for the ratio data. Also, the slope was closer to one (0.82 ± 0.02), and the intercept was closer to zero (11 ± 1).

A comparison was made between ^{133}Xe and ^{99m}Tc-HMPAO after vasodilation with Diamox in a subset of subjects. Subjects receiving Diamox had an average global CBF (^{133}Xe) increase of 20 ± 2 ml/min/100 g (25%). Profile plots showing a close relationship in one subject and a weak relationship in another subject are provided in Figures 4A and 4B, respectively. The relative distribution of the two radiopharmaceuticals averaged across subjects studied after Diamox is shown in Figure 4C. Again, there is agreement in the general pattern of relative distribution after Diamox. No statistically significant differences were found across regions for all subjects ($p = 0.53$). Neither were there differences for individual regions ($0.005 < p > 0.99$).

Regression analysis of ^{99m}Tc-HMPAO count density ratios and rCBF ratios after Diamox showed only a moderate correlation ($r = 0.66$), a modest slope (0.43) and a large intercept (0.58) (Fig. 5A). rCBF and derived ^{99m}Tc-HMPAO rCBF data (Fig. 5B) had a better correlation ($r = 0.77$), slope (0.61 ± 0.04) and intercept (31 ± 3) relative to the Diamox ratio regression analysis.

Regression analysis of the combined Diamox and baseline ratio data yielded a correlation ($r = 0.72$) that was slightly less than the baseline regression (0.78), while slope (0.51 ± 0.03) and intercept ($b = 0.51 \pm 0.08$) were unchanged from the baseline-only regression. Similarly, regression analysis comparing rCBF to derived ^{99m}Tc-HMPAO rCBF was not different from the baseline data ($r = 0.90$, $m = 0.81 \pm 0.02$, $b = 13.6 \pm 2$).

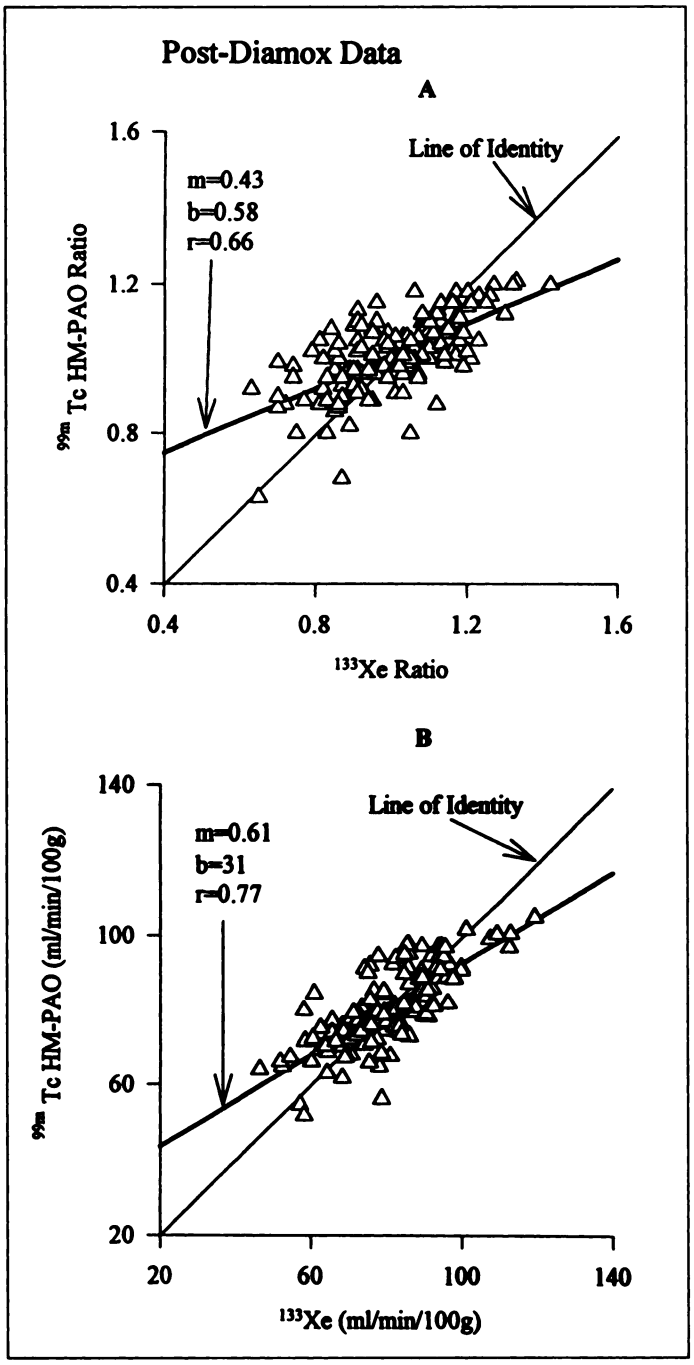

FIGURE 5. (A) Linear regression analysis after Diamox comparing ^{99m}Tc-HMPAO count density ratios to rCBF ratios or (B) comparing derived ^{99m}Tc-HMPAO rCBF (ml/min/100 g) to rCBF (ml/min/100 g, ^{133}Xe).

DISCUSSION

Profile analysis of baseline data revealed eight ROIs with significant differences between the distributions of ^{133}Xe and ^{99m}Tc-HMPAO. Although the magnitude of these differences was small, in each case ^{133}Xe showed greater contrast (higher peaks and lower valleys). The distribution across regions for all subjects was not significantly different between ^{133}Xe and ^{99m}Tc-HMPAO ($p = 0.52$). There was a linear relationship between ^{99m}Tc-HMPAO count density and ^{133}Xe rCBF ratios, but with a slope ($m = 0.52$) substantially less than one and a positive intercept ($b = 0.48$). This may indicate that ^{99m}Tc-HMPAO underestimates high flow and overestimates low flow.

These results are in agreement with studies of rCBF ratios measured by PET (^{15}O CO_2 inhalation method) compared to ^{99m}Tc-HMPAO count density ratios, that show an overestimation of low and an underestimation of high rCBF (*5,11*). Andersen et al. also showed that a curvilinear relationship existed between ^{133}Xe rCBF ratios and ^{99m}Tc-HMPAO count density ratios in patients with a variety of neurological disorders (*3*). It has been suggested that the underestimation of high rCBF by ^{99m}Tc-HMPAO is a consequence of backdiffusion from brain to blood (*3,4*).

The use of ratio data may in itself exaggerate an unfavorable comparison between ^{133}Xe and ^{99m}Tc-HMPAO. Our study (and many others) showed that gCBF varies substantially from subject to subject (44 to 81 ml/min/100 g in our data). Consequently, data ratioed to gCBF leads to an overlap of areas with potentially markedly different absolute rCBF. For example, a ratio of 0.9 could represent 80 ml/min/100 g in one individual and 50 in another. Conversely, regions with the same absolute rCBF could be associated with very different ratio values because of a difference in gCBF.

Linearization models for ^{99m}Tc-HMPAO have been developed by other investigators to correct for backdiffusion and address limitations of ratio data (*3-5,11*). We instead used a ratio between ^{133}Xe gCBF and ^{99m}Tc-HMPAO global count density as a simple scaling factor to estimate ^{99m}Tc-HMPAO rCBF values. The comparison between ^{99m}Tc-HMPAO derived rCBF and ^{133}Xe rCBF shows a much closer correlation ($r = 0.92$), with a slope closer to one and an intercept closer to zero (Fig. 3B). These values are comparable to the correlation coefficients, slopes and intercepts shown by linearization methods (*3,5,11*). Whether ^{99m}Tc-HMPAO rCBF values are corrected using linearization or our method, there is still mild underestimation of rCBF at high flow. We found that the underestimation of high rCBF occurs between 60–80 ml/min/100 g, which is similar to our previous studies using dual-isotope imaging (*12*). Inugami et al. showed that ^{99m}Tc-HMPAO underestimated CBF beginning at 30–50 ml/min/100 g compared to PET rCBF (*5*).

The comparison between ^{133}Xe and ^{99m}Tc-HMPAO mimics our comparison between ^{133}Xe and ^{99m}Tc ECD. Because the data for these two studies were collected identically, we have provided a crossover comparison. For either ratio data (Fig. 6A) or derived rCBF (Fig. 6B), there was little difference between ^{99m}Tc-HMPAO and ^{99m}Tc ECD. In contrast, in single-pass extraction studies, Di Rocco et al. (*16*) showed that ^{99m}Tc-HMPAO CBF correlated better than ^{99m}Tc ECD CBF measured by microspheres. Two explanations can be offered regarding the differences in our results. First, the ratio calibration method we used will overestimate the closeness of the fit between rCBF (^{133}Xe) and derived rCBF since gCD is forced to equal gCBF for each subject. Second, and more importantly, the experiment of Di Rocco et al. does not account for effects of backdiffusion due to their rapid post-injection sampling method, which are present in our measurements. Both ^{99m}Tc ECD and ^{99m}Tc-HMPAO have limited first pass extraction and underestimate high rCBF because of backdiffusion (*13-17*). Murase et al. (*15*) showed that ^{99m}Tc-ECD backdiffusion was significantly less than that of ^{99m}Tc-HMPAO. At the same time, Di Rocco et al. and others have shown ^{99m}Tc ECD has a lower extraction fraction (especially at higher rCBF) than ^{99m}Tc-HMPAO (*4,15,16*). Our data, illustrating no net difference between the two agents relative to ^{133}Xe rCBF, implies that the differences between extraction fraction (favoring HMPAO) and backdiffusion (favoring ECD) approximately cancel out over the range of normal rCBF.

To estimate the effects of high flow on ^{99m}Tc-HMPAO uptake, seven patients received injections of the vasodilator Diamox, producing a 25% increase in gCBF. This is similar to

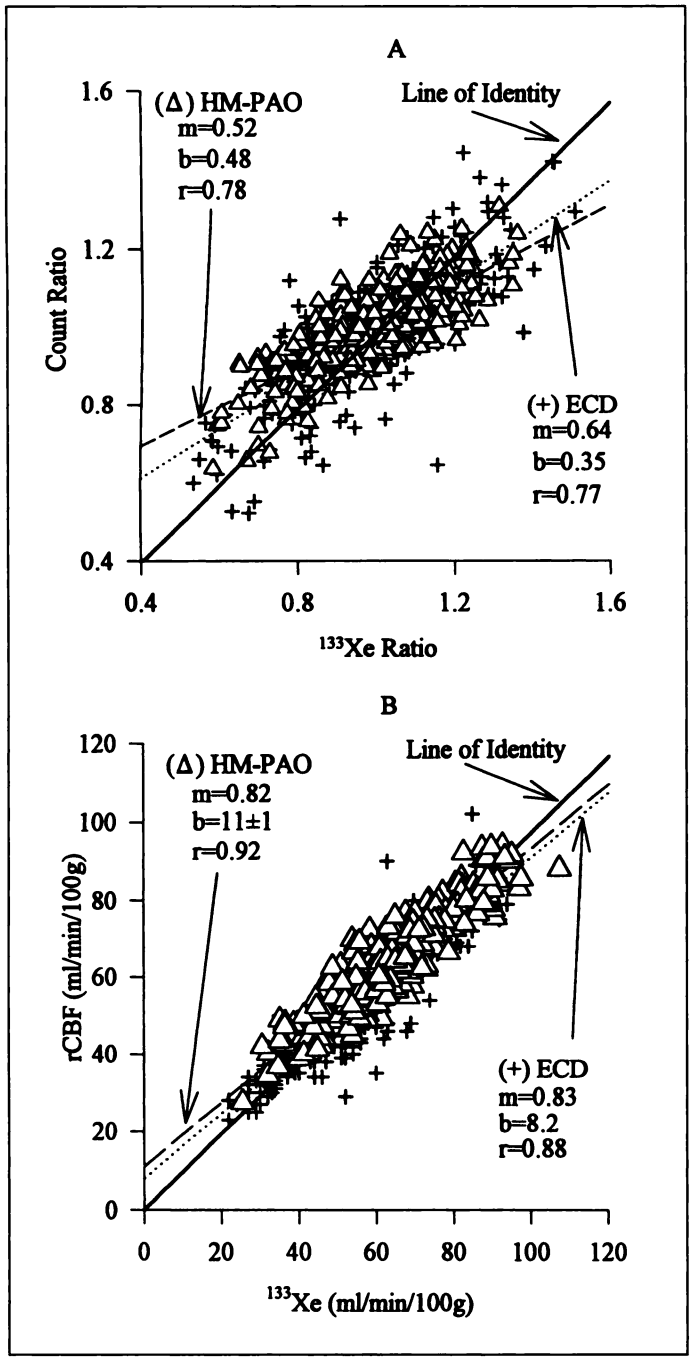

FIGURE 6. (A) Linear regression analysis comparing ^{99m}Tc-HMPAO (- - .) and ^{99m}Tc ECD (. . . . .) count density ratio to rCBF (^{133}Xe) ratio, or (B) comparing derived ^{99m}Tc-HMPAO rCBF (ml/min/100 g, - - .) and derived ^{99m}Tc-ECD rCBF (ml/min/100 g, ...) to rCBF (ml/min/100 g, ^{133}Xe).

the mean Diamox-induced gCBF increase (30%) found by Bonte et al. (*18*). Other investigators have reported that the increase in ^{99m}Tc-HMPAO uptake after Diamox ranges between 10%–40% (*19-21*). We found general agreement between rCBF (^{133}Xe) ratios and ^{99m}Tc-HMPAO count density ratios after Diamox (Fig. 4C). However, linear regression analysis showed that both ratio and derived rCBF data after Diamox (Fig. 5) had a poorer correlation, slope and intercept than for baseline data.

It is possible that the weaker correlation between rCBF and derived ^{99m}Tc-HMPAO rCBF after Diamox relative to baseline was due to the fewer number of subjects analyzed. Therefore, a comparison was made between the baseline studies of the seven patients who received Diamox and the baseline of all 19 subjects in this study. There were no significant differences between the baseline rCBF regression (r = 0.89), slope (m = 0.75) and intercept (b = 15) of the seven subjects receiving Diamox and the baseline rCBF regression data of all 19 subjects studied. Therefore, the reduced correlation between derived ^{99m}Tc-HMPAO rCBF and rCBF after Diamox is not a consequence of smaller sample size. It is most likely that the 20 ml/min/100 g increase in gCBF after Diamox, which should aggravate backdiffusion phenomena, led to a decrease in the correlation between ^{133}Xe and ^{99m}Tc-HMPAO. It is important to keep in mind that the reduction in correlation was not severe, and the combined baseline and Diamox data indicated good overall relationship. Also, Matsuda et al. and Burt et al. have reported that ^{99m}Tc-HMPAO is effective at estimating changes in rCBF after a Diamox challenge (*19,20*).

CONCLUSION

This study shows that ^{99m}Tc-HMPAO generally follows the distribution pattern of rCBF (^{133}Xe). The correlation between rCBF (^{133}Xe) and derived ^{99m}Tc-HMPAO rCBF suggests a closer relationship than ratio data, although there is still evidence that ^{99m}Tc-HMPAO mildly underestimates high rCBF. Further, greater underestimation of high rCBF was shown in patients after Diamox. Both ratio and derived rCBF data suggest nearly identical relationships between ^{99m}Tc-HMPAO and ^{99m}Tc ECD relative to true rCBF over the range of normal resting cerebral blood flow.

ACKNOWLEDGMENTS

We thank Drs. F.J. Bonte and R.F. Leroy for assisting with subject recruitment. This research was supported in part by a grant from Amersham/Medi-Physics.

REFERENCES

1. Devous MD, Payne JK, Lowe JL, Leroy RF. Comparison of ^{99m}Tc-ECD to ^{133}Xe SPECT in normal controls and in patients with mild-to-moderate regional cerebral blood flow abnormalities. *J Nucl Med* 1993;34:754–761.
2. Neirinckx RD, Canning LR, Piper IM, et al. Technetium-99m-d,l-HMPAO: a new radiopharmaceutical for SPECT imaging of regional cerebral blood perfusion. *J Nucl Med* 1987;28:191–202.
3. Andersen AR, Friberg HH, Schmidt JF, Hasselbalch SG. Quantitative measurements of cerebral blood flow using SPECT and [^{99m}Tc]-*d,l*-HMPAO compared to ^{133}Xe. *J Cereb Blood Flow Metab* 1988;8:S69–S81.
4. Lassen NA, Andersen AL, Friberg L, Paulson OB. The retention of [^{99m}Tc]-d,l-HMPAO in human brain after intracarotid bolus injection: a kinetic analysis. *J Cereb Blood Flow Metab* 1988;8:S13–S22.
5. Inugami A, Kanno I, Uemura K, et al. Linearization correction of ^{99m}Tc-labeled hexamethyl-propylene amine oxime (HMPAO) image in terms of regional CBF distribution: comparison to $C^{15}O_2$ inhalation steady-state method measured by positron emission tomography. *J Cereb Blood Flow Metab* 1988;8:S52–S60.
6. Stokely EM, Sveinsdottir E, Lassen NA, Rommer P. A single-photon dynamic computer assisted tomograph (DCAT) for imaging brain function in multiple cross sections. *J Comp Assist Tomogr* 1980;4:230–240.
7. Kanno I, Lassen NA. Two methods for calculating regional cerebral blood flow from emission computed tomography of inert gas concentrations. *J Comput Assist Tomogr* 1979;3:71–76.
8. Celsis P, Goldman T, Henriksen L, Lassen NA. A method for calculating regional cerebral blood flow from emission computed tomography of inert gas concentrations. *J Comput Assist Tomogr* 1981;5:641–645.
9. Smith GT, Stokely EM, Lewis MH, Devous MD, Bonte FT. Error analysis of the double-integral method for calculating brain blood perfusion from inert gas clearance data. *J Cereb Blood Flow Metab* 1984;4:61–67.
10. Stokely EM, Totah J, Homan R, Devous MD, Bonte FT. Interactive graphics methods for regional quantification of tomographic brain blood flow images. *IEEE Proceedings Medcomp* 1982;316–318.
11. Yonekura Y, Nishizawa S, Mukai T. SPECT with [^{99m}Tc]-d,l-hexamethyl-propylene amine oxime (HMPAO) compared with regional cerebral blood flow measured by PET: effects of linearization. *J Cereb Blood Flow Metab* 1988;8:S82–S89.
12. Devous MD Sr, Payne JK, Lowe JL. Dual-isotope brain SPECT imaging with ^{99m}Tc and ^{123}I: clinical validation using xenon-133 SPECT. *J Nucl Med* 1992;33:1919–1924.
13. Léveillé J, Demonceau G, Walovitch RC. Intrasubject comparison between ^{99m}Tc-ECD and ^{99m}Tc-HMPAO in healthy human subjects. *J Nucl Med* 1992;33:480–484.
14. Tsuchida T, Nishizawa S, Yonekura Y, et al. SPECT images of ^{99m}Tc-ethyl cysteinate dimer in cerebrovascular diseases: comparison with other cerebral perfusion tracers and PET. *J Nucl Med* 1994;35:27–31.

15. Murase K, Tanada T, Inoue Y, et al. Kinetic behavior of ^{99m}Tc-ECD in the human brain using compartment analysis and dynamic SPECT: comparison with ^{99m}Tc-HMPAO. *J Nucl Med* 1992;33:909.
16. Di Rocco RJ, Silva DA, Kuczynski BL, et al. The single-pass cerebral extraction and capillary permeability-surface area product of several putative cerebral blood flow imaging agents. *J Nucl Med* 1993;34:641–648.
17. Walovitch RC, Hill TC, Garrity ST, et al. Characterization of ^{99m}Tc-l,l-ECD for brain perfusion imaging. Part 1: pharmacology of ^{99m}Tc-ECD in nonhuman primates. *J Nucl Med* 1989;30:1892–1901.
18. Bonte FJ, Devous MD Sr, Reish JS. The effect of acetazolamide on regional cerebral blood flow in normal human subjects as measured by SPECT. *Invest Radiol* 1988;23:564–568.
19. Matsuda H, Higashi S, Kinuya K, et al. SPECT evaluation of brain perfusion reserve by the acetazolamide test using ^{99m}Tc-HMPAO. *Clin Nucl Med* 1991;16: 572–579.
20. Burt RW, Witt RM, Cikrit D, Carter J. Increased brain retention of ^{99m}Tc-HMPAO following acetazolamide administration. *Clin Nucl Med* 1991;16:568–571.
21. Knop J, Thie A, Fuchs C, Siepmann G, Zeumer H. ^{99m}Tc-HMPAO SPECT with acetazolamide challenge to detect hemodynamic compromise in occlusive cerebrovascular disease. *Stroke* 1992;23:1733–1742.

Optimal Number of Views in 360° SPECT Imaging

ZongJian Cao, Lawrence E. Holder and Charles C. Chen
Department of Diagnostic Radiology and the Cancer Center, University of Maryland Medical Center, Baltimore, Maryland

This study examined SPECT-reconstructed image quality as a function of the number of views, and determined the minimum number of views necessary to remove aliasing artifacts in 360° SPECT. **Methods:** Computer simulation was performed using a two-dimensional Shepp-Logan head phantom and a high-resolution parallel-beam collimator with and without photon attenuation. **Results:** In 360° SPECT, aliasing artifacts were reduced by changing the number of views from an even number 16 to its neighboring odd numbers 15 or 17, from 32 to 31 or 33 and from 64 to 63 or 65. Image quality of 15 or 17 views, 31 or 33 views and 63 or 65 views was similar to that of 32, 64 and 128 views, respectively. **Conclusion:** Replacing an even number of views by its neighboring odd numbers in 360° SPECT significantly decreased aliasing artifacts. Thirty-one or 33 views are sufficient to remove most of the aliasing artifacts in 360° SPECT with a matrix of 64 × 64 pixels. This method can be applied to fast 360° SPECT since fewer views are used.

Key Words: SPECT; image reconstruction; aliasing artifact

J Nucl Med 1996; 37:1740–1744

In SPECT, artifacts resulting from insufficient sampling of data appear as streaks and star-shaped patterns in the reconstructed images and are called aliasing artifacts. Insufficient data may occur due to undersampling of projection data by using too coarse an acquisition matrix or by acquiring an insufficient number of views. To avoid aliasing, the number of views in 180° parallel-beam SPECT should be approximately equal to the number of rays in each projection (*1*). For example, a 180° SPECT study with a 64 × 64 matrix requires 64 views. For 360° SPECT studies, it is usually assumed that the number of views should be doubled compared to 180° SPECT to avoid aliasing artifacts (*2*). This assumption has been applied to clinical imaging (*3*). In this study, we examined the possibility of reducing the number of views in 360° SPECT without creating significant aliasing artifacts.

We investigated the effects of the number of views on reconstructed image quality in both 360° and 180° SPECT. Since it was not possible to use odd numbers of views on existing SPECT systems, the studies were conducted with computer simulation. Photon attenuation is the most important physical factor in SPECT, so we evaluated its effect on image quality as an independent factor.

Received June 30, 1995; revision accepted Oct. 18, 1995.
For correspondence or reprints contact: ZongJian Cao, PhD, Department of Diagnostic Radiology, University of Maryland Medical Center, 22 South Greene St., Baltimore, MD 21201-1595.

MATERIALS AND METHODS

Simulated projection data were generated in an analytical approach with a two-dimensional Shepp-Logan head phantom using a high-resolution parallel-beam collimator. The head phantom is composed of six ellipses of different positions, orientations, sizes and activities (*4*).

For 360° SPECT, we simulated 15, 16, 17, 31, 32, 33, 63, 64, 65 and 128 views with an array of 64 pixels per view. For 180° SPECT, 16, 17, 32, 33, 64 and 65 views were used, and the detector moved counter-clockwise from left lateral to right lateral along the anterior half of a circular orbit.

For 360° SPECT, data were simulated with and without attenuation and for 180° SPECT, only with attenuation. In the simulations with attenuation, two attenuation coefficients were used for the inside of the head phantom. One was the water attenuation coefficient (0.15/cm) and another was 0.2/cm. The latter was used to simulate attenuation effects inside a larger object (such as a chest) with the water attenuation coefficient. As an initial investigation, photon scatter and statistical noise were not included. All reconstructed images were normalized to the same total number of counts.

A parallel-beam collimator allows detection of oblique projection rays, restricted by the acceptance angle of the collimator. The acceptance angle was set to be 2.7° which was representative of most commercially available high-resolution parallel-beam collimators.

A previously developed analytical simulation method (*5*) was used to generate the projection data. The method is more efficient than Monte Carlo simulation techniques. In generating the data, the intersecting length of a projection ray within an elliptical object in the phantom was obtained by solving for the equations of the ray and ellipse and was used to calculate the contribution of activity from the elliptical object and the attenuation along the ray towards the detector. The data were determined by the activity and attenuation.

Image reconstruction was performed using filtered backprojection without attenuation compensation. The reconstructed images had a matrix of 64 × 64 and a pixel size of 0.64 cm. The quality of the reconstructed images was evaluated both visually and quantitatively. Two quantitative methods were used, intensity profiles and mean squared deviations (MSDs) from true pixel values. The MSD was defined as

$$MSD = \frac{1}{N}\sum_{i=1}^{N}(p_i - P)^2, \qquad \text{Eq. 1}$$

where N is the total number of pixels within a region of interest (ROI), p_i is the pixel value of the ith pixel in the ROI, and P is the true pixel value. For a uniform ROI, P is a constant. Larger MSDs